Vol 12 No 9, September 2003
1009-1963/2003/12(09)/0955-09

Chinese Physics

© 2003 Chin. Phys. Soc.
and IOP Publishing Ltd

Magnetic guide of cold atoms using a U-shaped current-carrying conductor*

Liu Nan-Chun(刘南春)[b)†] and Yin Jian-Ping(印建平)[a)b)]

[a)] *State Key Laboratory for Optical and Magnetic Resonance Spectroscopy, Department of Physics, East China Normal University, Shanghai 200062, China*

[b)] *Department of Physics, Suzhou University, Suzhou 215006, China*

(Received 14 October 2002; revised manuscript received 30 April 2003)

We propose a new scheme to magnetically guide cold neutral atoms using a U-shaped current carrying conductor. The spatial magnetic field distribution from the U-shaped current-carrying conductor and the relationship between the magnetic field and parameters of the U-shaped conductor are analysed. Our study shows that U-shaped current-carrying conductor can be used to realize single- or double-channel magnetic guiding of cold atoms in weak-field-seeking states and to construct various atom-optical elements. By using Monte Carlo simulations, the dynamic process of the guided atomic-beam splitting in an atomic-beam splitter composed by the U-shaped current-carrying conductor is studied, and some results are presented.

Keywords: U-shaped current-carrying conductor, single-channel magnetic guide, double-channel magnetic guide, atom-optical elements

PACC: 3510, 3345B, 5255K, 3280P

1. Introduction

For the past few years, an increasing interest has been focused on the fields of miniaturized atomic traps and guides, because these devices can be applied in some experiments such as low-dimensional quantum gases or the construction of integrated atom-optical circuits. Various types of atomic guides, such as optical and magnetic guides, etc., have been proposed, in which atomic guides based on the interaction between optical field and atoms were first proposed and developed, such as, laser guides based on a single red-detuned Gaussian laser beam,[1−3] and optical guides based on a blue-detuned evanescent wave in hollow fibre,[4−6] and on a blue-detuned dark hollow beam.[7,8]

However, among the various approaches, the atomic guides based on the interaction between magnetic fields and atoms are more attractive for some reasons. In contrast to optical guides, the inevitable heating due to the photon recoil can be avoided. Magnetic guides can also offer excellent stable environment that some experiments require. Moreover, cold atoms in magnetic guides are easily manipulated because the field configuration can be changed conveniently during the experiments by adjusting electric current. Atom guiding scheme using magnetic field has been proposed by Hau[9] and was first demonstrated by Schmiedmayer experimentally.[10,11] Afterwards, various magnetic guiding schemes using current-carrying wires or permanent magnets have been proposed and demonstrated.[12−31] Different magnetic-field configurations can be used to guide cold atoms either in strong- or weak-field-seeking states. It is well known that those guiding schemes using current-carrying wires are popular because the magnetic field can be changed easily by adjusting the electric current in the wires. So a magnetic guiding device using current-carrying conductors with various shapes has more benefits because the generated magnetic field can be altered either by changing the electric current in the conductor or by changing the shape and its parameters of the conductor.

*Project supported by the National Natural Science Foundation of China (Grant Nos 69878019 and 10174050), the Natural Science Foundation of Jiangsu Province, China (Grant Nos DK97139 and 00KJB140001), and the Fostering Foundation of New-Century Academic Leader from the Education Bureau of Jiangsu Province, China.

†Corresponding author. E-mail: xqluo@suda.edu.cn

In this paper, we propose such a scheme to guide cold neutral atoms using a static magnetic field generated by a U-shaped current-carrying conductor (UCCC). This scheme can form a controllable single- or double-channel guide, which is adaptable and practical in different experimental studies, and can be used to construct various atom-optical elements, such as the atomic funnel, atomic beamsplitter, and atom interferometer, etc. In section 2, we derive the equations for calculating the magnetic field from a UCCC. In section 3, we calculate the magnetic-field distribution produced by the UCCC and analyse the relations between the magnetic field and some parameters. In section 4, some atom-optical elements composed of UCCC are proposed and discussed. The main conclusion and outlook are summarized in the final section.

2. Magnetic guiding scheme and its principle

It is well known that the magnetic field generated by electric current can be calculated by using Ampere's circuital law. Our proposed magnetic guiding scheme is shown in Fig.1. In this scheme, the magnetic guiding tube with a zero axial magnetic field is provided by a UCCC with two sides a (here we take the sides a=5mm unless otherwise indicated.) vertical to the bottom b and an electric current I propagating along the z-axis. For the convenience of calculation, we assume that the U-shaped conductor is infinite long in the z-direction, and a small homogeneous bias field along the z-direction to prevent Majorana spin-flips is not considered. From Ampere's circuital law, we can derive the expression to calculate the spatial distribution of the magnetic field from the UCCC, and the x and y components of the magnetic field are expressed as, respectively,

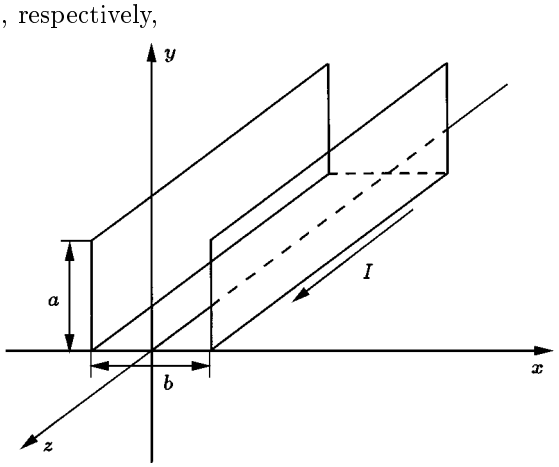


Fig.1. Schematic diagram of atomic magnetic guiding using the UCCC with current I, side height a, and bottom width b.

$$\begin{aligned} B_x =& \frac{\mu_0 I}{2\pi(2a+b)}\left\{\left[\arctan\left(\frac{-b/2-x}{y}\right)\right.\right. \\ & \left.- \arctan\left(\frac{b/2-x}{y}\right)\right] \\ & + \frac{1}{2}\{-\log[(2x-b)^2+4y^2] \\ & + \log[4(y-a)^2+(2x-b)^2] \\ & - \log[(2x+b)^2+4y^2] \\ & \left.+ \log[4(y-a)^2+(2x+b)^2]\}\right\}, \end{aligned} \tag{1}$$

$$\begin{aligned} B_y =& \frac{\mu_0 I}{2\pi(2a+b)}\left\{\left\{\arctan\left[\frac{(a-y)}{(x-b/2)}\right]\right.\right. \\ & \left.+ \arctan\left[\frac{y}{(x-b/2)}\right]\right\} \\ & + \left\{\arctan\left[\frac{(a-y)}{(x+b/2)}\right]\right. \\ & \left.\left.+ \left[\frac{y}{(x+b/2)}\right]\right\} + \frac{1}{2}\{-\log[(x-b/2)^2+y^2]\right. \\ & \left.+ \log[(x+b/2)^2+y^2]\}\right\} \end{aligned} \tag{2}$$

and then a magnitude of the total magnetic field is given by

$$|B| = \sqrt{B_x^2 + B_y^2}. \tag{3}$$

When an atom with an atomic magnetic dipole moment μ moves in a static inhomogeneous field B, it will experience a position-dependent interaction potential due to Zeeman effect. We assume that the motion of laser-cooled atoms in the magnetic field is adiabatic, that is, the projection of the atomic angular momentum on to the magnetic field direction remains constant. In this case, the interaction potential that the atoms experience in the magnetic field is given by

$$U_{\rm mag} = -\boldsymbol{\mu}\cdot\boldsymbol{B} = m_F g_F \mu_{\rm B} \boldsymbol{B}, \tag{4}$$

where m_F is the magnetic quantum number, g_F is the Lande g-factor and $\mu_{\rm B}$ is the Bohr magneton. When $\boldsymbol{\mu}\cdot\boldsymbol{B} > 0$, the atoms in a strong-field-seeking state will feel an attractive potential and can be guided along the maximum of the magnetic field.[12] If $\boldsymbol{\mu}\cdot\boldsymbol{B} < 0$, the atoms in a weak-field seeking state will experience a repulsive potential and can be guided along the minimum of the magnetic field.[14–17] For ^{87}Rb atoms in the $|F=2, m=2\rangle$ state, which is a weak-field-seeking state, the trapping potential is given by

$$U_{\rm mag} = 6.72\times 10^5 |\boldsymbol{B}| \quad (\mu{\rm K}), \tag{5}$$

where the unit of the magnetic field B is Tesla. The corresponding gradient force of the magnetic field on cold atoms becomes

$$F = \nabla(\mu B) = -m_F g_F \mu_B \nabla|B|. \quad (6)$$

Thus, the weak-field-seeking atoms ($m_F g_F > 0$) will be repelled towards the minimum of the magnetic field by the gradient force F and guided along the z-axis.

3. Theoretical calculations and analysis

From Eqs.(1)–(5), we calculate the spatial distribution of trapping potential for ^{87}Rb atoms generated by the UCCC, and the results are shown in Figs 2(a) and (b). It can be found from Fig.2(a) that there is a point of zero magnetic field, whose coordinate position is at (x_0, y_0). Thus, the magnetic field will form a magnetic tube with an axial line of $|B|$=0 and can be used to guide cold atoms in a weak-field-seeking state along the z-direction. From Fig.2(b), however, it is surprised to find that there are two points of zero magnetic field ($x_\pm$, y_0). Making a comparison between Figs 2(a) and (b), we see that only the bottom width b of the U-shaped conductor is changed. For the convenience of analysis, the side height a of the conductor and current I are fixed, and a shape parameter β is defined as

$$\beta = b/a. \quad (7)$$

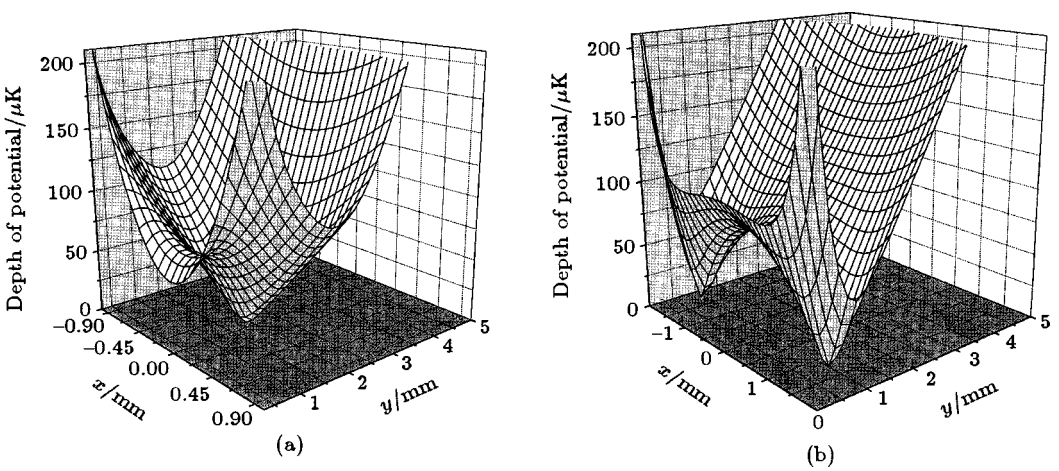


Fig.2. The trap potential of the UCCC in the x-y plane: (a) single-channel magnetic guide for I=10A, a=5mm, and β=0.4; (b) double-channel guide for I=10A, a=5mm, and β=0.8.

From Eqs.(1)–(3), we investigate how the change of β causes splitting of the magnetic guiding channel. We calculate the distributions of magnetic field B in the x-direction (at y_0) for different β, and the results are shown in Fig.3(a). In the case of β=0.2 and 0.4, there is only a single-channel guiding centre at x=0. When β is continuously increased from 0.6 to 1.0, a potential barrier at x=0 will be bulged and two guiding centres will be formed, and the distance between the two guiding centres will be increased with β. This results in a controllable double-channel magnetic guiding. Figure 3(b) shows the distributions of magnetic field B in the y-direction (at x_0 or $x_\pm$) for different β. We can see from Fig.3(b) that the position y_0 of the guiding centre is decreased as β is increased. However, when β is greater than a certain value, y_0 is only changed slightly. So we need only to consider the change of guiding central positions $x_\pm$ in the x-direction with β.

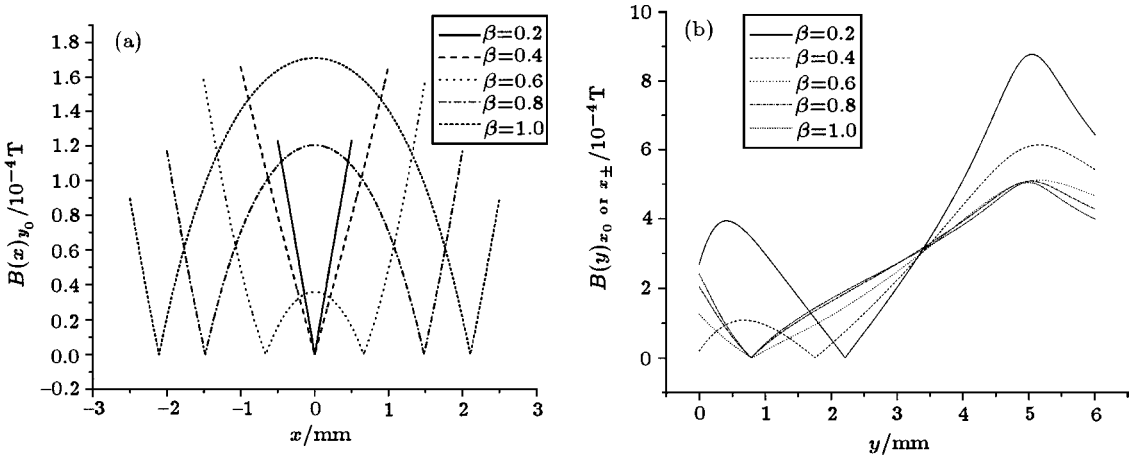


Fig.3. (a) The distributions of magnetic field B in the x-direction at y_0 for different β values; (b) the distributions of magnetic field B in the y-direction at x_0 or $x_\pm$ for different β values.

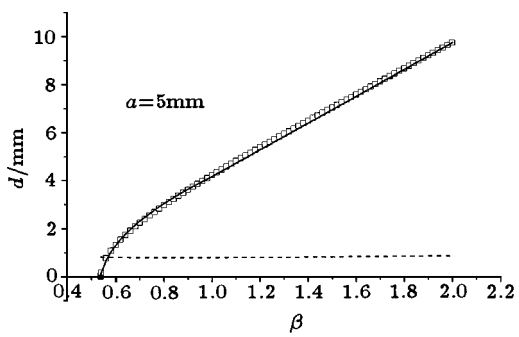


Fig.4. Relationship between d (the distance between the two points of zero magnetic field) and β=b/a. Squares are the calculated values and the solid line is the fitted curve using Eqs.(8a) and (8b), and the dashed line shows the change of position y_0.

If we define the distance between two guiding centres as d, then d=0 shows that the guide is a single channel; if $d > 0$, the guide is a double-channel. We also calculate the relationship between β and d, and the result is shown in Fig.4. It is clear from Fig.4 that when $\beta \leq 0.5389$, d=0. This shows that there is only a single guiding centre. While if $\beta > 0.5389$, $d > 0$. This shows that a single magnetic guide will be split into two magnetic ones with increasing β. We can also find from Fig.4 that the distance d increases with β, and there is an approximately linear relationship between d and β for $\beta > 1.0$, whereas there is a nonlinear relationship between d and β for $0.5389 < \beta < 1.0$. From the above analysis, the relationship between d and β can be described by equations as follows

$$d = A_1 + \sqrt{A_2 + A_3\beta} \quad (\text{mm}) \quad (\beta \leq 1), \qquad (8a)$$

$$d = A_4 + A_5\beta \quad (\text{mm}) \quad (\beta \geq 1), \qquad (8b)$$

where A_1, A_2, A_3, A_4 and A_5 are five fitting parameters. (In the case of a=500μm, $A_1 = -0.446039$, $A_2 = -24.1032$, $A_3 = -45.3036$, $A_4 = -1.38674$ and $A_5 = 5.54509$.) From the analysis mentioned above, we can see that the proposed UCCC can be used to realize a single-channel atomic magnetic guide or a controllable double-channel guide. This shows that the UCCC is applicable to construct various atom optical elements, such as atomic funnel and atomic beamsplitter, etc.

From Eq.(3), we can find another property of the UCCC. That is, the magnetic field from the UCCC is directly proportional to electric current I, and inversely proportional to characteristic parameter β of the UCCC. So we can easily change the potential-well depth by changing the current I or parameter β in the experiment. When the current I is higher, and the β of UCCC is smaller, the transverse confinement for the cold atoms will be tighter, and then the mean transverse moving range of the guided atoms in the magnetic potential tube generated by the UCCC will become very narrow. Especially, when this transverse size is close to the de Broglie wavelength of the guided cold atoms, it seems hopeful to realize a single-mode matter waveguide under certain conditions. Based on the above analysis, our atomic guiding scheme using the UCCC is adaptable to guide cold atoms in a wider range of temperature.

4. Construction of atom optical elements

The advances of guiding technique have stimulated significant interest in atom optical elements, which have wide and important applications in the experiments with cold atoms or cold atomic beams.

In this section, we will discuss the potential applications of our UCCC in atom optics and present some interesting and practical atom-optical devices.

4.1. Atomic funnel

In section 3, we have mentioned that decreasing the geometric parameter β of the UCCC will cause a tighter transverse confinement for cold atoms under the condition of identical current I. This property can be used to design an atomic funnel, as shown in Fig.5, in which, (a) and (b) are the three-dimensional (3D) view and 2D vertical view of atomic funnel, respectively, and (c) is the corresponding B-field contours or atomic funnel potentials. To keep the single-channel guiding mode, β should be fixed at a value smaller than 0.5389 as the bottom width b decreases. This requires that the side height a of the UCCC should be linearly decreased with the linear reduction of the bottom width b. We can find from Fig.5(c) that when the sizes (a, b) of the UCCC are linearly decreased, the radius of the magnetic-field contour with an identical value will be reduced. This shows that it is possible to realize the transformation of atomic waveguiding modes from a multimode state to a single-mode one in our funnel as the part of the UCCC below the cross section (C) satisfies the condition of single-mode waveguide.

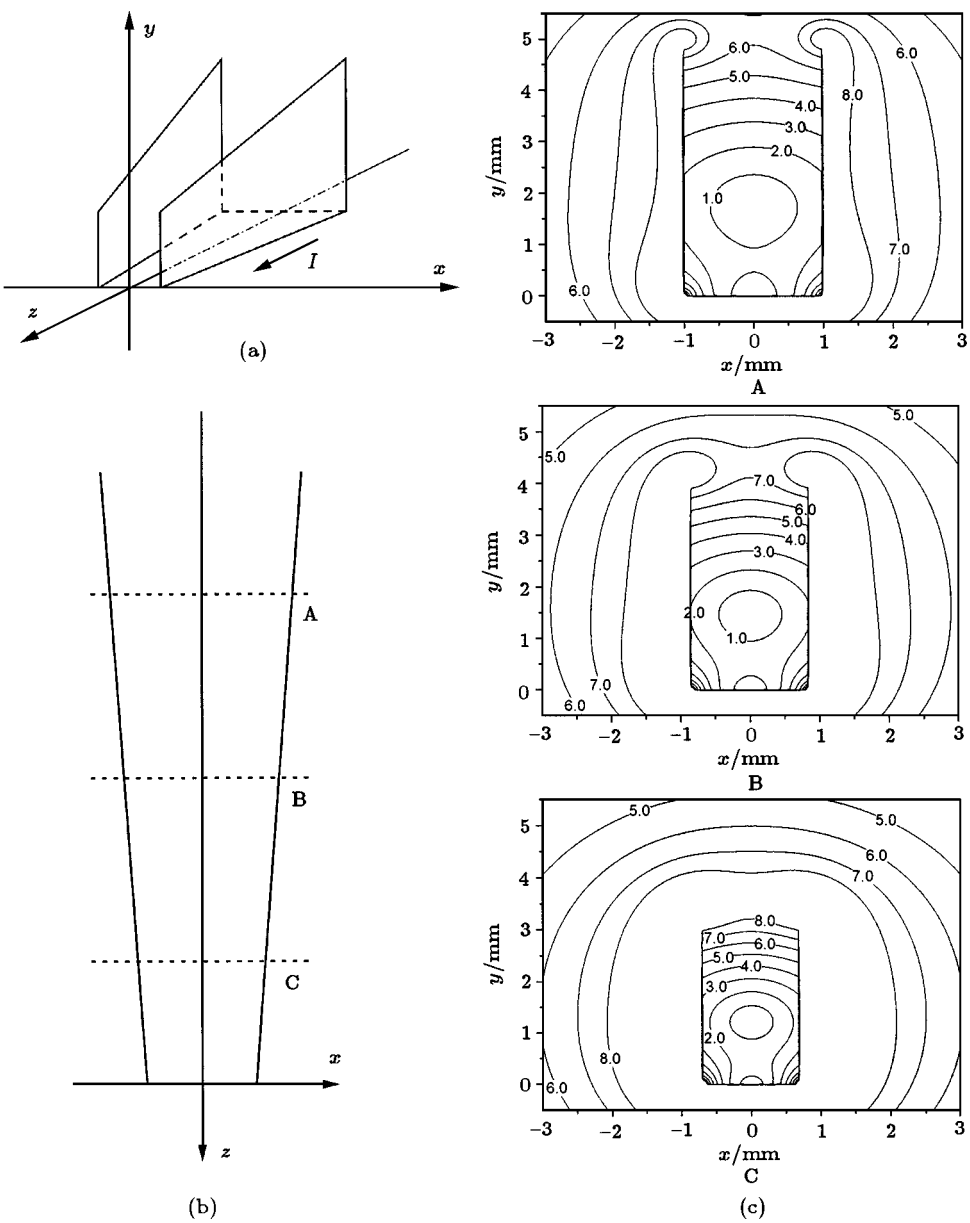


Fig.5. The schematic of atomic funnel based on the UCCC. 5(a) and 5(b) are the 3D and 2D views of the funnel respectively. 5(c) shows the corresponding magnetic contours, which are drawn at 1×10^{-4}T intervals and the first contour shows 1×10^{-4}T. The current I=10A.

4.2.Atomic beamsplitter

We have found in section 3 that a single magnetic potential tube can be split into two naturally with increasing β. Based on this special property, we propose a scheme of atomic beamsplitter as shown in Fig.6 (a). In order to clearly show the working principle of this atomic beamsplitter, we present a series of contours at different positions along the z-axis,

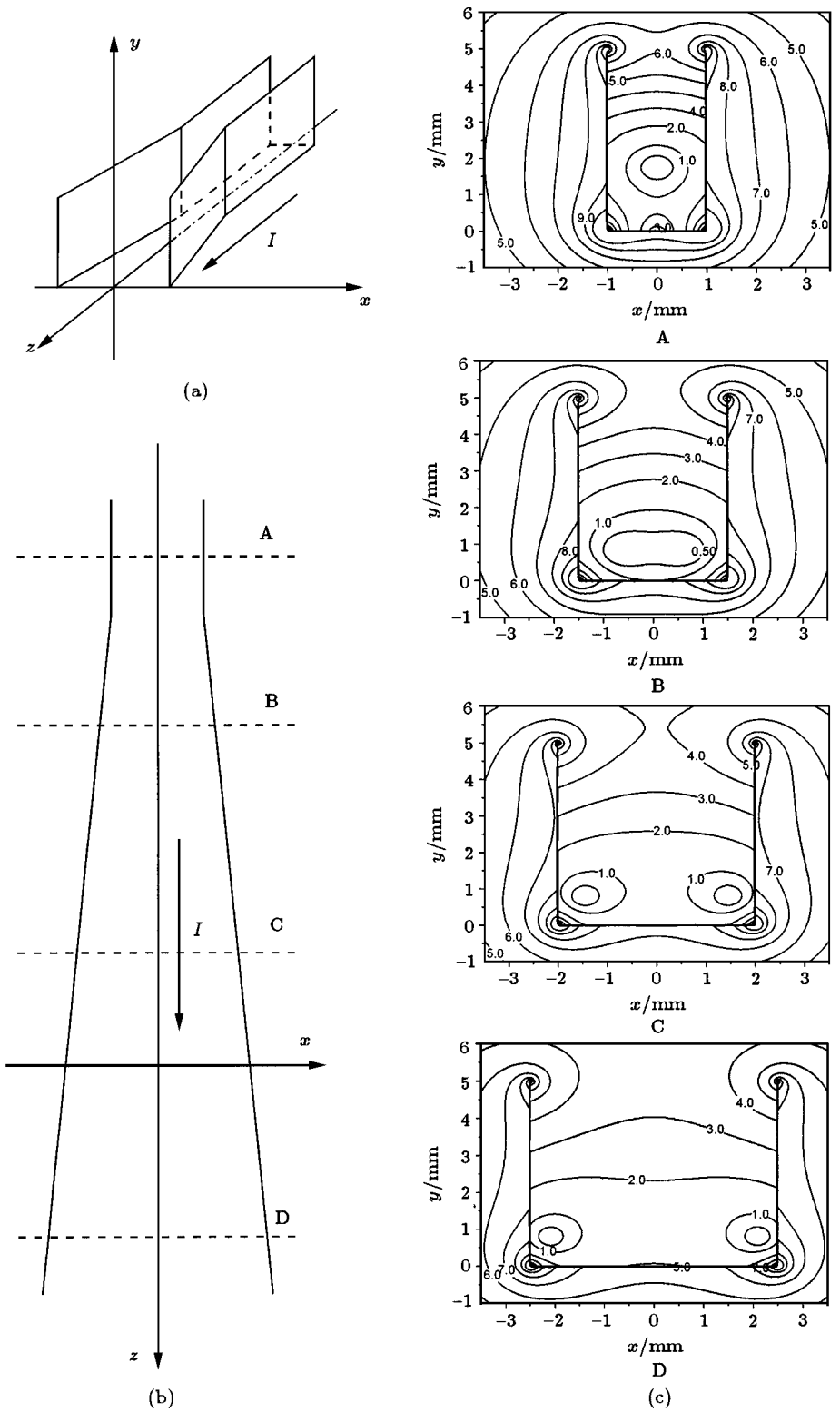


Fig.6. The schematic of atomic beamsplitter formed by the UCCC. 6(a) and 6(b) are the 3D and 2D views of beamsplitter respectively. 6(c) shows the corresponding magnetic contours at (A) β=0.4; (B) β=0.6; (C) β=0.8; (D) β=1.0. Contours are drawn at 1×10^{-4}T intervals and the first contour shows 0.5×10^{-4}T. The current I=10A and side height a=5mm.

that is, at different β, which are shown in Figs 6(b) and (c). From these figures, we can understand how a single-channel magnetic guide is split into a double-channel one with increasing β. As compared with a previous scheme of atomic beam-splitting based on V-shaped current carrying conductor,[30] no bias magnetic fields are needed (in our previous scheme using the VCCC, these bias fields are used to shift two guiding centres back to their self-centre of two output arms). So the atomic beamsplitter proposed here is simpler and much convenient for some experiments with cold atomic beams.

We have also studied the dynamical process of atomic-beam splitting and atom distribution in the output-plane for different conditions by using classical Monte Carlo simulations, and the results are shown in Fig.7. In the simulations, the atomic beamsplitter formed by the UCCC is placed vertically, and we assume that under the action of the gravity force, the cold atoms from a magnetic-optical trap of 30μK are released and loaded into the input channel of the beamsplitter, and the simulation parameters used are a=5mm, β =0.4–1.0 and z=0–15mm. In this case, the guided cold-atom beam is split by 50%–50%. In Figs 7(a)–(c), the corresponding current I is 50, 75 and 100A, respectively. It is clear from Fig.7 that besides most of cold atoms are guided along the two output channels, some atoms with high energy appear between the two output guiding centres, as shown in Fig.6(c). This is because the atoms with high energy can overcome the potential barrier between the two guiding centres in the x-direction (where the magnetic potential is much lower than the other parts, as shown in Fig.2(b)) and go back and forth. With increasing current I from 50 to 100A, i.e. the potential barrier between the two guiding centres being increased, the atomic number appearing between the two output guiding centres will be decreased greatly.

4.3.Atom interferometer

We can also combine two atomic beam-splitters, as shown in Fig.5 (a), to set up an atom interferometer, which is shown in Figs 8 (a) and (b), the corresponding magnetic field or potential contours are shown in Fig.8(c). It is clear from Fig.8(c) that the magnetic potential of this interferometer are completely symmetric, which can ensure coherent splitting at the first splitting point, coherent superposition at the second splitting point, and coherent propagation in the two magnetic guiding channels between the two splitting points. So this interferometer may be used to realize the single-mode atom interference based on the mode-keeping capability of the UCCC atomic beam-splitter, which have been explained in section 4.1.

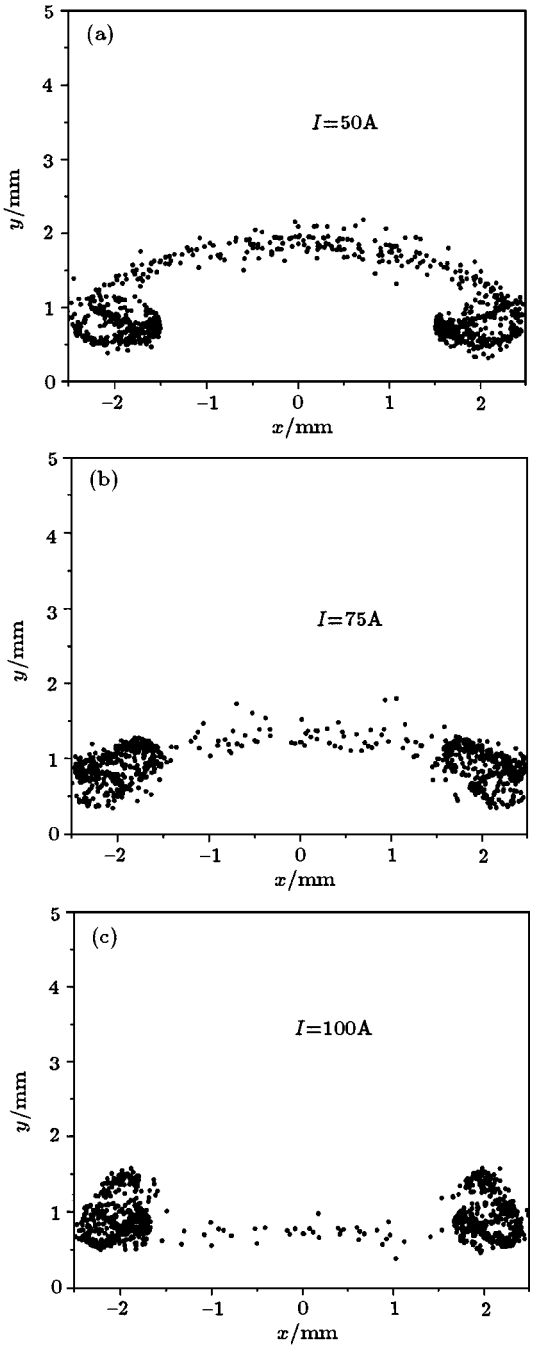


Fig.7. Simulation results of atom distribution at the two outlets of atomic beamsplitter for different currents I.

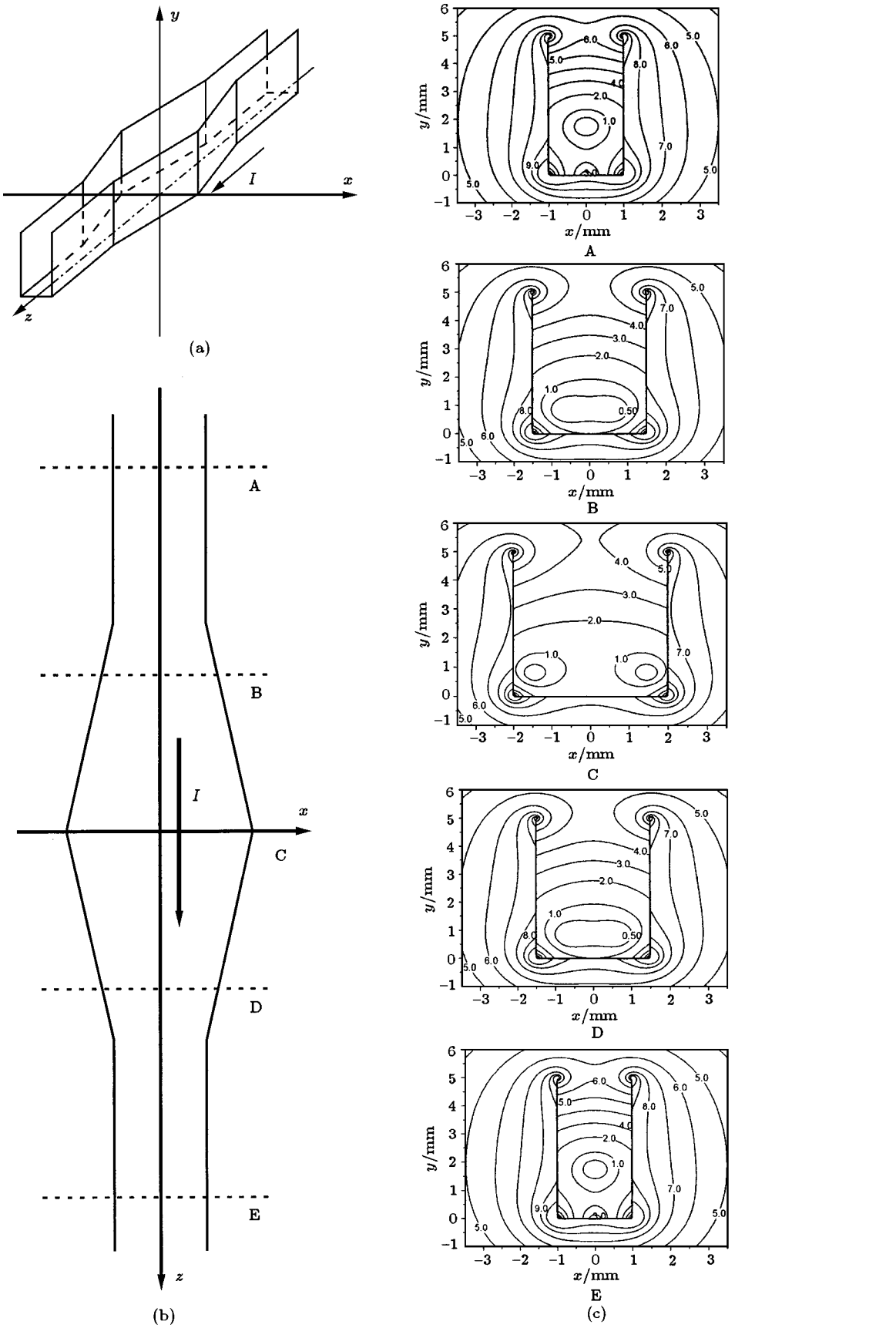


Fig.8. The schematic of atom interferometer based on the UCCC. 8(a) and 8(b) are the 3D and 2D views of the interferometer respectively. 8(c) illustrates the corresponding magnetic contours, which are drawn at 1×10^{-4}T intervals and the first contour shows 0.5×10^{-4}T. The current I=10A and side height a=5mm.

More complex manipulation or control of cold atoms or cold atomic beams can be realized in the experiment by using the UCCC scheme. Also, we can integrate the proposed atom optical elements on an atom chip to perform some research on integrated atom optics. For example, we can combine an atomic funnel (which can be used to collect cold atoms from a magnetic-optical trap), together with an atom guide and an atom microtrap to realize a micro-well Bose–Einstein condensate and then to generate an atom laser and realize the coherence propagation of atom laser beams for some applications on an atom chip.

5. Conclusions and outlook

In this paper, an atomic guiding scheme based on the interaction between week-field-seeking atoms and a static magnetic field generated by the UCCC has been proposed. We have calculated the spatial distribution of the magnetic field from the UCCC and studied the relationship between the magnetic field and the geometrical parameters of the U-shaped conductor, and found that when the parameter β <0.5389, there is only a single magnetic guiding channel in the UCCC, while for β >0.5389, there are two magnetic guiding channels. So when β is continuously increased from a value smaller than 0.5389 to 1.0, the UCCC can be used to realize a controllable double-channel guide, even to form various atom optical elements, such as atomic funnel, atomic beamsplitter and atom interferometer, and so on.

We have also performed Monte Carlo simulations to study the dynamic process of atomic beam splitting in our beamsplitter and found that when the current in the conductor is high enough, the guided cold atoms can be completely confined within two output guiding channels of the beamsplitter. Our study shows that the atomic beamsplitter and its atom interferometer proposed here are better than our previous ones based on the V-shaped current carrying conductor[30] because no bias fields are needed. So these atom optical elements cannot only be integrated to construct atom chips, but also used to study some basic physical problems, such as, atomic holography, atom interference quantum computer and information processing, and so on.

References

[1] Pruvost L *et al* 1999 *Opt. Commun.* **166** 199
[2] Ol'shanii M A *et al* 1993 *Opt. Commun.* **98** 77
[3] Renn M J *et al* 1995 *Phys. Rev. Lett.* **75** 3253
[4] Marksteiner S *et al* 1994 *Phys. Rev.* A **50** 2680
[5] Renn M J *et al* 1996 *Phys. Rev.* A **53** R648
[6] Ito H *et al* 1996 *Phys. Rev. Lett.* **76** 4500
[7] Yin J P *et al* 1998 *Phys. Rev.* A **58** 509
[8] Yin J P *et al* 1997 *Opt. Commun.* **138** 287
[9] Hau L V *et al* 1995 *Phys. Rev. Lett.* **74** 3138
[10] Schmiedmayer J 1995 *Phys. Rev.* A **52** R13
[11] Schmiedmayer J 1995 *Appl. Phys.* B **60** 169
[12] Denschlag J *et al* 1999 *Phys. Rev. Lett.* **82** 2014
[13] Müller D *et al* 1999 *Phys. Rev. Lett.* **83** 5194
[14] Deforer N H *et al* 2000 *Phys. Rev. Lett.* **84** 1124
[15] Key M *et al* 2000 *Phys. Rev. Lett.* **84** 1371
[16] Fortagh J *et al* 2000 *Appl. Phys.* B **70** 701
[17] Yin J P *et al* 2001 *J. Chin. Chem. Soc.* **48** 555
[18] Geoepfert A *et al* 1999 *Appl. Phys.* B **69** 217
[19] Li D *et al* 1999 *Opt. Commun.* **160** 72
[20] Richmond J A *et al* 1998 *Acta Phys.* **48** 481
[21] Xu L *et al* 2002 *Opt. Commun.* **188** 93
[22] Rowlands W J *et al* 1996 *Opt. Commun.* **126** 55
[23] Myatt C J *et al* 1997 *Phys. Rev. Lett.* **78** 586
[24] Forttagh J *et al* 1998 *Phys. Rev. Lett.* **81** 5310
[25] Reichel J *et al* 1999 *Phys. Rev. Lett.* **83** 3398
[26] Zobay O *et al* 2000 *Opt. Commun.* **178** 93
[27] Cassettar D *et al* 2000 *Appl. Phys.* B **70** 721
[28] Cassettar D *et al* 2000 *Phys. Rev. Lett.* **85** 5483
[29] Muller D *et al* 2000 *Opt. Lett.* **25** 1382
[30] Liu N *et al* 2002 *Eur. Phys. J.* D **19** 137
[31] Yin J P *et al* 2002 *Chin. Phys.* **11** 472